LITHOLOGICAL INTERPRETATION OF MARTIAN CRUSTAL SEISMIC VELOCITIES FROM INSIGHT. B. Knapmeyer-Endrun[1], J. Li[2], D. Kim[3], A.-C. Plesa[4], S. McLennan[5], E. Hauber[4], R. Joshi[6], J. Shi[7], C. Beghein[2], M. Wieczorek[7], M.P. Panning[8], P. Lognonné[7], W. B. Banerdt[8] [1]Bensberg Observatory, University of Cologne, Germany (bknapmey@uni-koeln.de), [2]Department of Earth, Planetary, and Space Sciences, University of California, Los Angeles, CA, USA, [3]Institute of Geophysics, ETH Zurich, Zurich, Switzerland, [4]Institute of Planetary Research, German Aerospace Center (DLR), Berlin, Germany [5]Department of Geosciences, Stony Brook University, Sony Brook, NY, USA, [6]Max Planck Institute for Solar System Research, Göttingen, Germany [7]Université Paris Cité, Institut de physique du globe de Paris, CNRS, Paris, France [8]Jet Propulsion Laboratory, California Institute of Technology, Pasadena, CA, USA

Introduction: Analysis of data from the seismometer SEIS [1] on NASA's InSight mission [2] has provided a wealth of information on the crustal structure of Mars, both beneath the lander [3-11] and for other locations on the planet [12-16]. Here, we collect all P- and S-wave velocity information for kilometer-scale crustal layers available and compare it with parameters predicted by rock physics models to guide the interpretation in terms of crustal lithology. A similar approach has previously only been attempted for crustal SV-wave velocities below the lander [17,18] and P- and SV-wave velocities in the shallowest 200 meters of the subsurface beneath InSight [19].

InSight Data: Information on the crustal structure and specifically crustal SV-wave velocities at the landing site has been derived from Ps- and PPs-receiver functions [3-7] and complemented by P-wave velocity information from vertical component autocorrelations [4,8,9]. These data are consistent with a three-layer crust of around 43 ± 5 km thickness beneath the lander, with markedly low velocities in the uppermost two layers extending to 10 and 20 km depth, respectively. Independent observations of SsPp reflections [10] and SH reverberations [11] provide complementary additional constraints on P-wave and SH-wave velocities, respectively, of the top-most 10 km of the crust beneath SEIS. Meanwhile, a recent receiver function analysis of events with higher frequency content found evidence for another slow layer comprising the uppermost approximately 2 km of the subsurface at the landing site [12].

Information on average crustal S-wave velocities away from the lander is based on the dispersion analysis of surface waves of two big impacts [13], and the largest marsquake recorded by InSight, S1222a, which excited not only fundamental mode Rayleigh waves, but also Love waves, higher modes, and multi-orbit surface waves [14-16]. These data are consistent with higher SV-wave velocities of around 3.2 km/s in the upper 25-30 km of the crust, as compared to the landing site, whereas velocities at larger depth seem to agree. The question whether the SV-wave velocities between 5 and 30 km depth are the same in the highlands and lowlands [14] or the velocities are higher in the highlands, approaching 3.5 km/s [16], is still under debate.

Finally, P- and SV-wave velocities in the uppermost 20 km of the crust at a location far from InSight are constrained by PP- and SS-precursors of the most distant marsquake located by InSight, S0976a [17]. They are broadly consistent with results for the landing site, with a somewhat thinner uppermost layer that might also be present along the minor arc path from S1222a to InSight [14]. Fig. 1 summarizes the crustal velocity information.

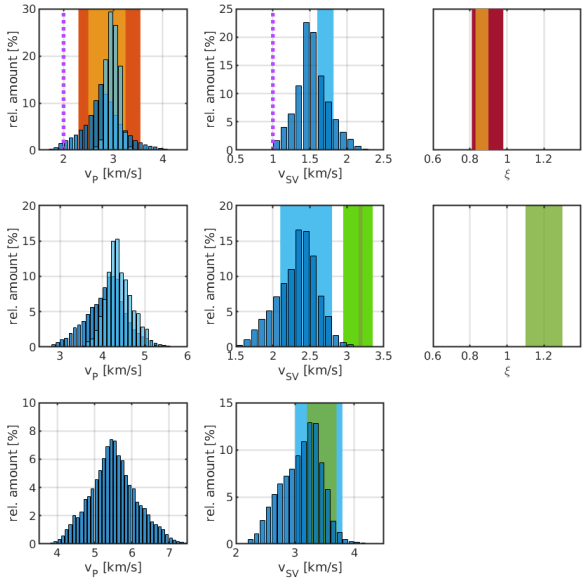

Figure 1: Constraints on seismic velocities in crustal layers 1 (top) to 3 (bottom). Dark blue [4] and light blue [7] refer to receiver function results, and red colors to results from analysis of other phases [10,11] for structure below the lander. Green refers to surface wave results averaging over larger areas of the planet [13-15]. Dashed vertical lilac lines in top row refer to results for an approximately 2 km thick surficial layer below the lander [12].

Modeling: Following previous studies [18-20], we consider poorly consolidated and cemented sediments

as well as cracked rocks with various pore fillings to model the measured seismic velocities. We use the Hertz-Mindlin model for unconsolidated or poorly consolidated sediments [21], Dvorkin and Nur's cemented-sand model for consolidated sediments [22], the self-consistent approximation by Berryman [23] for elliptical inclusions of arbitrary aspect ratios to simulate cracked rocks, and Gassmann fluid substitution [24] to study the effect of liquid water in each case. Considered lithologies include basalt, andesite, dacite, kaolinite, and plagioclase, with pores filled by either CO_2 or water, and cementation due to calcite, gypsum, halite and ice.

Results: The bulk properties of the top-most 2 km of the subsurface below InSight as estimated by [12] can be modeled with either unconsolidated basaltic sands, or clay with a low amount (2%) of cementation, consistent with previous inferences from geology [25]. Cracked basalt, dacite or clay could potentially also explain the data. Within the range of lithologies considered, the seismic velocities can neither be explained by intact rocks, nor rocks with completely filled pores, e.g. by ice, nor by fluid-saturated rocks.

The seismic P- and SV-velocities to about 10 km depth beneath InSight could independently be modeled by somewhat cemented basaltic sediments (e.g. 2% halite or 10% ice), but would require very low v_P/v_S ratios, of less than 1.5, that are inconsistent with receiver function inversions [7]. Rather, both P- and SV-wave velocities are consistent with fractured basaltic rocks or plagioclase of at least 5% porosity, depending on crack aspect ratios. About 10% of that porosity needs to have a preferred orientation to explain the observed anisotropy [11]. Again, the velocities are too low for intact rocks or rocks with ice-filled pores. However, the S-wave velocities are too high for any of the other lithologies considered (dacite, andesite, kaolinite). For porosities exceeding 12%, the measured velocities would also be consistent with water-saturated rocks. At least partially water-filled pores or some mixing with andesite, dacite or plagioclase would also increase v_P/v_S ratios, which for the basaltic dry rock model are low (1.6 or less).

The transition to higher velocities at about 10 km depth beneath InSight can be modeled by more intact material, i.e. a porosity reduction by 50% compared to the layer above, which can be achieved by either cementation or a lower initial porosity. The SV-velocities derived by surface waves down to 25-30 km depth are consistent with basalts with a porosity of less than 5% or nearly intact plagioclase. They could also be explained by rocks with a higher porosity if pores are filled by ice. However, the depth range over which the surface waves indicate nearly constant velocities is inconsistent with the depth extent of the Martian cryosphere away from the poles of less than 15 km, even under the most favorable conditions (high freezing temperature and crustal thermal conductivity) [26]. While the wide-spread presence of ice to 25-30 km depth is thus unlikely, ice near the surface could potentially erase traces of the low velocities observed to 10 km depth beneath InSight and possibly at another location close to the equator [17]. Since the presence of water does not influence the S-wave velocities, it cannot be constrained based on the surface wave data.

The velocities at larger depth, i.e. below about 20 km beneath InSight and 25-30 km along the surface wave paths, are consistent with intact basalt, as are the v_P/v_S ratios derived from receiver function inversions.

Acknowledgments: The InSight seismic waveform data are available from the IPGP Datacenter, NASA-PDS and IRIS-DMC [27,28].

References: [1] Lognonné P. et al. (2019) *Space Sci Rev, 215*, 12. [2] Banerdt W.B. et al. (2020) *Nature Geoscience, 12*, 183-189. [3] Lognonné P. et al. (2020) *Nature Geoscience, 13*, 213-220. [4] Knapmeyer-Endrun B. et al. (2021) *Science, 373*, 438-443. [5] Kim D. et al. (2021) *JGR, 126*, e2021JE006983. [6] Duran et al. (2022), *PEPI, 325*, 106851. [7] Joshi R. et al. (2022), *Authorea*, 10.1002/essoar.10512135.1 [8] Compaire N. et al. (2021) *JGR, 126*, e2020JE006498. [9] Schimmel M. et al. (2021) *Earth Space Sci., 8*, e2021EA001755. [10] Li J. et al. (2022) *Earth Space Sci.*, e2022EA002416. [11] Li J. et al. (2022) *EPSL, 593*, 117654. [12] Shi J. et al (2023) *accepted by GRL* [13] Kim D. et al. (2022) *Science, 378*, 417-421. [14] Kim D. et al. (2022) *GRL, 49*, e2022GL101666. [15] Beghein C. et al. (2022) *GRL, 49*, e2022GL101508. [16] Li J. et al. (2022) *GRL, 49*, e2022GL101243. [17] Li J. et al. (2022) *Nat Commun, 13*, 7950. [18] Manga M. and Wright V. (2021) *GRL, 48*, e2021GL093127. [19] Kilburn R. et al. (2022) *JGR, 127*, e2022JE007539. [20] Wright V. et al. (2022) *GRL, 49*, e2022GL099250. [21] Mindlin, R.D. (1949) *J Appl Mech, 16*, 259-268. [22] Dvorkin, J. and Nur, A. (1996) *Geophysics, 61*, 1363-1370. [23] Berryman, J.G. (1980) *J Ac Soc Am, 68*, 1820-1831. [24] Gassmann, F. (1951) *Vierteljahresschr. Naturfor. Gesell. Zürich, 96*, 1-23. [25] Pan, L. et al. (2020) *Icarus, 338*, 113511. [26] Plesa, A.-C. et al. (2020), *EPSC2020-698*. [27] InSight Mars SEIS Data Service, SEIS raw data, InSight Mission. IPGP, CNES, ETHZ, ICL, MPS, ISAE-Supaero, LPG, MFSC (2019), 10.18715/SEIS/INSIGHT.XB.2016. [28] InSIght Mars SEIS Data Service, InSight SEIS Data Bundle. PDS Geosciences (GEO) Node (2019), 10.17189/1517570.